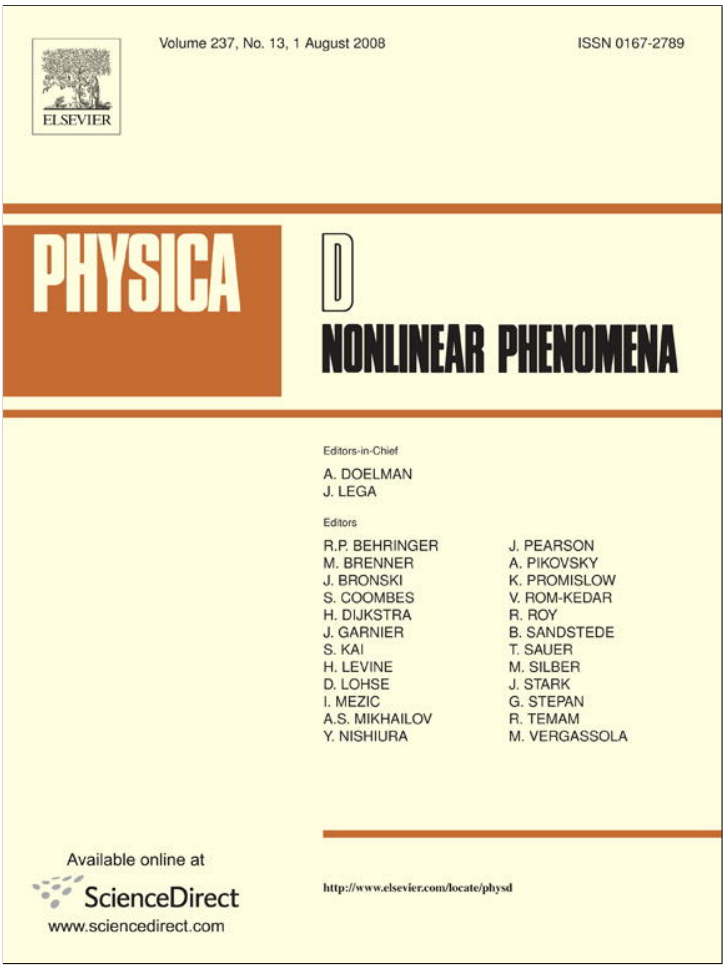

Available online at www.sciencedirect.com
ScienceDirect
Physica D 237 (2008) 1689–1704
PHYSICA D
www.elsevier.com/locate/physd

Compound windows of the Hénon-map

Edward N. Lorenz*

Department of Earth, Atmospheric, and Planetary Sciences, Massachusetts Institute of Technology, Cambridge, MA 02139, USA

Received 5 December 2006; received in revised form 15 November 2007; accepted 23 November 2007
Available online 3 December 2007

Communicated by B. Sandstede

With great sadness, we note the passing away of Edward Lorenz, who opened up a revolutionary new field of science, and led the way through it for many, many years.

Abstract

For the two-parameter second-order Hénon map, the shapes and locations of the periodic windows – continua of parameter values for which solutions $x_0, x_1, \ldots$ can be stably periodic, embedded in larger regions where chaotic solutions or solutions of other periods prevail – are found by a random searching procedure and displayed graphically. Many windows have a typical shape, consisting of a central "body" from which four narrow "antennae" extend. Such windows, to be called *compound windows,* are often arranged in bands, to be called *window streets,* that are made up largely of small detected but poorly resolved compound windows.

For each fundamental subwindow – the portion of a window where a fundamental period prevails – a stability measure U is introduced; where the solution is stable, $|U| < 1$. Curves of constant U are found by numerical integration. Along one line in parameter space the Hénon-map reduces to the one-parameter first-order logistic map, and two antennae from each compound window intersect this line. The curves where $U = 1$ and $U = -1$ that bound either antenna are close together within these intersections, but, as either curve with $U = -1$ leaves the line, it diverges from the curve where $U = 1$, crosses the other curve where $U = -1$, and nears the other curve where $U = 1$, forming another antenna. The region bounded by the numerically determined curves coincides with the subwindow as found by random searching. A fourth-degree equation for an idealized curve of constant U is established.

Points in parameter space producing periodic solutions where $x_0 = x_m = 0$, for given values of m, are found to lie on Cantor sets of curves that closely fit the window streets. Points producing solutions where $x_0 = x_m = 0$ and satisfying a third condition, approximating the condition that x_n be bounded as $n \to -\infty$, lie on curves, to be called *street curves* of order m, that approximate individual members of the Cantor set and individual window streets. Compound windows of period $m + m'$ tend to occur near the intersections of street curves of orders m and m'.

Some exceptions to what appear to be fairly general results are noted. The exceptions render it difficult to establish general theorems.

Keywords: Two-parameter maps; Periodic windows; Bifurcation curves

1. Introduction

Consider a dynamic system defined by equations that contain one or more parameters—quantities that are constant in any solution but may assume different constant values in different solutions. Let us restrict our attention to the "good" points in parameter space—simultaneous values of the parameters for which initial states chosen randomly from a bounded region of state space have a positive probability of producing solutions that remain bounded, i.e. do not blow up. Such points will be called *chaotic* if, after any initial states that produce blow-ups have been discarded, almost all remaining initial states produce chaotic solutions; they will be called *periodic* if, again after eliminating blow-ups, almost all initial states produce stable periodic solutions, or solutions that approach periodicity asymptotically, possibly after extended transient behavior resembling chaos. Points that fit neither category include some where intransitivity prevails, and chaos and periodicity can each be produced by a set of initial states

* Tel.: +1 617 253 4850; fax: +1 617 324 0308.
E-mail address: jmsloman@mit.edu.

0167-2789/$ - see front matter © 2007 Elsevier B.V. All rights reserved.
doi:10.1016/j.physd.2007.11.014

with positive measure. There may also be points where different initial states will produce different stable periodic or different chaotic solutions.

If one parameter is allowed to vary through a range while the others, if any, remain fixed, every point in the range will in some instances be chaotic. In other cases an otherwise chaotic range may be punctuated with periodic *windows*—one-dimensional continua of periodic points. Often there are infinitely many windows. Similarly, if several parameters are varied, there may be multidimensional windows. Such windows will constitute the subject of this work.

A system where chaotic points fill a range of a single parameter α is the frequently discussed (although not always named) tent map [7,10,13], sometimes written

$$X_{n+1} = \min(\alpha X_n, \alpha(1 - X_n)). \tag{1}$$

It is apparent that any point where $0 < \alpha < 2$ is good, and is chaotic if $\alpha > 1$; the single Lyapunov exponent is $\log \alpha$. A system with an infinity of windows is the logistic map, commonly written

$$X_{n+1} = \alpha X_n(1 - X_n); \tag{2}$$

it is probably the most intensively studied of all dynamical systems capable of chaotic behaviour. It is again apparent that any point where $0 < \alpha < 4$ is good; somewhat more effort is needed to show that chaotic and periodic points both abound when $\alpha > 3.5$. Studies of Eq. (2) date back at least to Julia [12], but they have proliferated only since the appearance of computers. May [16] has provided a particularly detailed exposition, and has tabulated the limiting values of α for the windows of small period. Each window consists of a continuum, which we shall call the principal *subwindow,* in which a solution with a fundamental period K is stable, followed without pause, as α increases, by continua of decreasing lengths, also qualifying as subwindows, where, for $n = 1, 2 \ldots$, period $2^n K$ is stable. Each window begins at a fold (saddle node) bifurcation point, while the successive subwindows are separated by flip (period doubling) bifurcations. A complete knowledge of the bifurcation structure therefore determines the locations of the windows and subwindows.

Feigenbaum [5] has shown that the successive lengths decrease by a factor that approaches a universal limit 4.6692. Following Feigenbaum and May we shall call these subwindows harmonics, even though they differ from the familiar musical harmonics in that the period rather than the frequency is a multiple of that of the fundamental. We have speculated [14], and Jakobson [11] has accomplished the rather involved task of proving, that even though any two chaotic values of α are separated by a window, the measure of the set of chaotic values is positive, while Collet and Eckmann [3] have established a similar result for a hybrid of the logistic and tent maps.

There are a number of algorithms for locating the windows of the logistic map, but their shapes have little choice but to be line segments. For systems with two or more parameters, however, explaining the shape of a window can present as big a problem as accounting for its location.

In this work we have chosen for study the map

$$X_{n+1} = Y_n + 1 - aX_n^2, \tag{3a}$$

$$Y_{n+1} = bX_n, \tag{3b}$$

introduced by Hénon [8] as the simplest dissipative second-order two-parameter polynomial system capable of producing chaos. The Lozi map [15]

$$X_{n+1} = Y_n + 1 - a|X_n|, \tag{4a}$$

$$Y_{n+1} = bX_n, \tag{4b}$$

which bears a relation to the Hénon map much like that of the tent map to the logistic map, seems equally simple, but its derivative possesses a discontinuity, which Hénon sought to avoid. As with the logistic map, Hénon-map windows may be divided into subwindows. A fold bifurcation curve forms one boundary of the principal subwindow, while the remaining subwindows are bounded by flip bifurcations.

In the following section we shall perform "brute force" numerical computations that will reveal in graphical form the locations and shapes in parameter space of numerous windows of the Hénon map. We shall find that many of the windows have similar shapes, and that their central portions tend to line up in bands. The task of the remaining sections will be to provide reasonable if not completely rigorous explanations for these findings.

2. Locating the windows by random searching

The present study was originally motivated by our desire to use the Hénon map to illustrate some of the basic properties of chaotic behaviour, particularly for an audience not especially familiar with chaos. A prerequisite for relevant numerical examples would appear to be a knowledge of what values of the parameters produce chaos; certainly values within a window must be avoided. This section is especially but by no means exclusively addressed to those who may wish to put the Hénon map to a similar use.

We first let $x_n = aX_n$ and then eliminate X_n and Y_n explicitly from Eqs. (3), obtaining the single equation

$$x_{n+1} = bx_{n-1} - x_n^2 + a. \tag{5}$$

An unspecified term in the sequence $x_0, x_1, x_2, \ldots$ produced by iteration from initial values x_0 and x_1 will simply be called an x. Use of x_n in place of X_n will simplify some of the derived equations.

In Figs. 1–3 that follow, each plotted point results from choosing a and b randomly from a uniform distribution over the area of the particular figure, choosing x_0 and x_1 randomly from uniform distributions between -2 and 2, and then examining the properties of the sequence of xs produced by iteration, plotting (a, b) if certain conditions are met. For these figures we have intentionally avoided using Eq. (5), or any relation derived from it, other than for producing the xs. If the sequences were something observed in nature instead of being generated

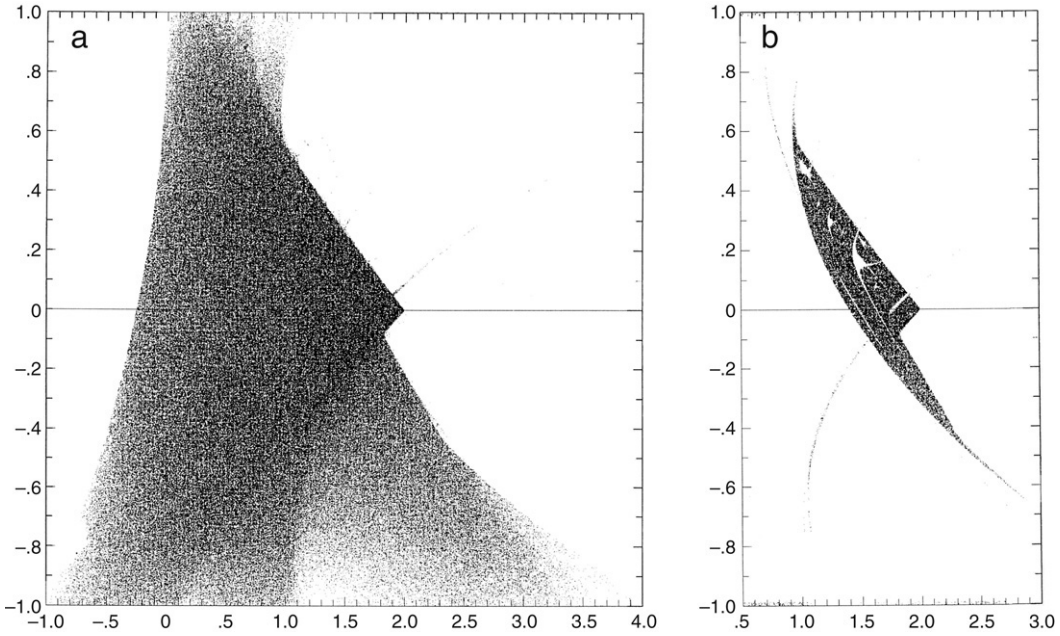

Fig. 1. (a) Locations (shaded) in parameter space where a solution of Eq. (5) has a positive probability of not blowing up, as determined by random searching. Variations in shading indicate variations in probability of a blow-up. Along horizontal line $b = 0$. (b) The same as Fig. 1(a), but for locations where a solution has a positive probability of being chaotic. Horizontal scales indicate a, vertical scales indicate b.

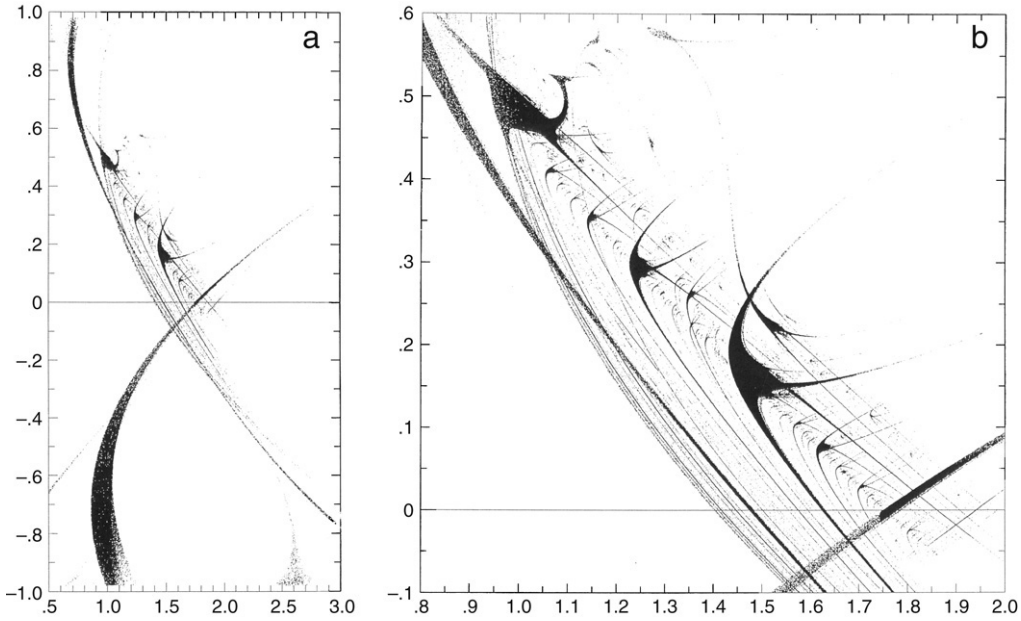

Fig. 2. (a) Same as Fig. 1(a), but for locations where a solution has a positive probability of being periodic. (b) An enlargement of a portion of Fig. 2(a). Horizontal scales indicate a, vertical scales indicate b.

by an equation, our approach would be considered empirical. It contrasts with the algebraic approach of Hitzl and Zele [8], who have presented bounding curves for the principal subwindows of period $K \leq 6$.

We first locate the good points; these are shown in Fig. 1(a). It is apparent that if $|b| > 1$, outside its range in the figure, Eq. (5) is an expanding mapping, and (a, b) is "bad" regardless of a. With $|b| < 1$ if, in iterating Eq. (5), $|x_n| > 10$ for some n, implying an imminent blow-up, we proceed immediately to the next choice of a, b, x_0, and x_1. If instead n reaches a chosen N and no blow-up has occurred, we plot (a, b) before proceeding to the next choice. In practice we have chosen $N = 300$, accepting the slight risk of a solution that blows up only after 300 iterations.

The variations in shading result from variations, as a and b vary, of the likelihood that the randomly chosen (x_0, x_1) will produce a blow-up. Some of the boundary curves continue inside as discontinuities in shading.

Fig. 1(b) shows the chaotic points. We assume a point to be chaotic and plot (a, b) if we fail to find a stable periodic

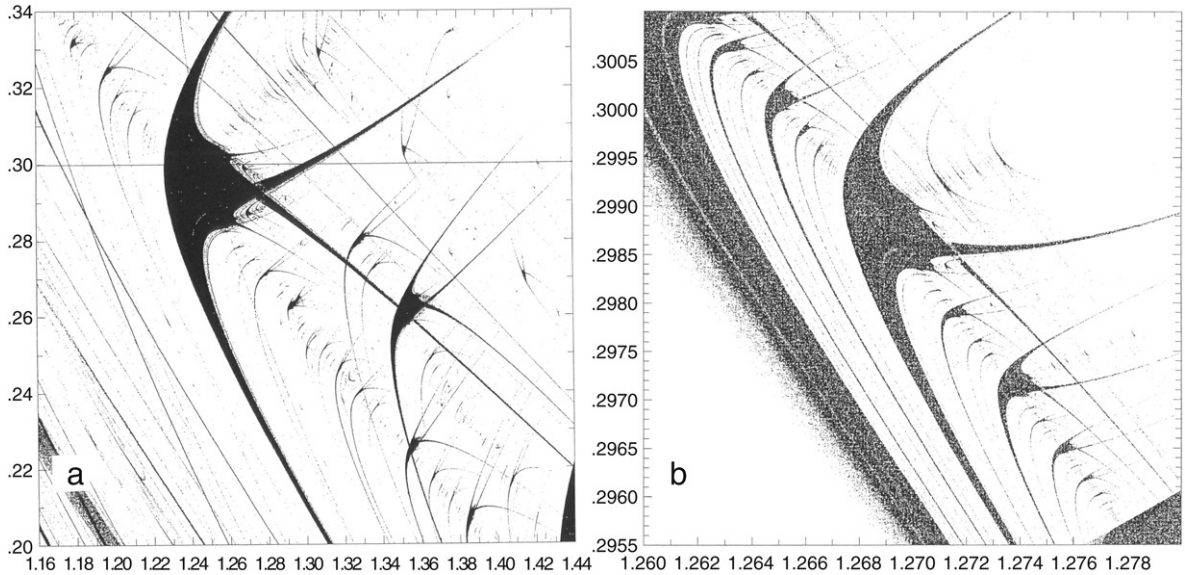

Fig. 3. (a) An enlargement of a portion of Fig. 2(b). Along horizontal line $b = 0.3$. (b) An enlargement of a portion of Fig. 3(a). Horizontal scales indicate a, vertical scales indicate b.

solution. To find solutions with periods not exceeding a chosen M, we choose ε and an integer J, and let $N = JM$. We again terminate the iteration if $|x_n| > 10$, but also, whenever $n = jM$ for some $j < J$, we note x_n and x_{n+1}, and if subsequently $|x_{n+K} - x_n| < \varepsilon$ and $|x_{n+1+K} - x_{n+1}| < \varepsilon$ for some $K < M$, i.e., if $|\Delta_0| < \varepsilon$ and $|\Delta_1| < \varepsilon$, where $\Delta_j = x_{n+j+K} - x_{n+j}$, we interrupt the process, and assume that we have approached a period-K solution. To test it for stability we perform $2K$ additional iterations, and evaluate Δ_K, Δ_{K+1}, Δ_{2K}, and Δ_{2K+1}. The matrix A governing the behaviour of small perturbations through K iterations satisfies

$$\begin{pmatrix} \Delta_K & \Delta_{2K} \\ \Delta_{K+1} & \Delta_{2K+1} \end{pmatrix} = A \begin{pmatrix} \Delta_0 & \Delta_K \\ \Delta_1 & \Delta_{K+1} \end{pmatrix}, \tag{6}$$

and its characteristic equation, with roots λ_1 and λ_2, is

$$(\Delta_0\Delta_{K+1} - \Delta_1\Delta_K)\lambda^2 - (\Delta_0\Delta_{2K+1} - \Delta_1\Delta_{2K})\lambda + (\Delta_K\Delta_{2K+1} - \Delta_{K+1}\Delta_{2K}) = 0, \tag{7}$$

and the solution is stable if $|\lambda_1| < 1$ and $|\lambda_2| < 1$. Here we accept the risk of missing a stable periodic solution where $K > M$, or one where $K < M$ but where there is transient chaotic behaviour lasting more than N iterations. Regions where solutions may be either chaotic or periodic will also appear shaded, but less heavily. In practice we let $\varepsilon = 0.00001$, while $M = 80$ and $J = 15$, so that $N = 1200$.

A few windows are plainly seen, but they prove to be more easily viewed if we reverse the shading, plotting periodic points, omitting those with period 1 or its harmonics to avoid obscuring certain other features. This is done in Fig. 2(a), where many more windows are detectable. In the curved band that widens near the lower left corner, period 3 or one of its harmonics is stable; the band that widens at the upper left is similarly produced by period 6. In the small weakly shaded area in the lower right, period 5 is stable. Each of these areas appears in a figure in [9]. In each case period 1 or 2 is also stable in the same area, so that intransitivity is present. Intransitivity is, in fact, a well-established feature of the Hénon map [4,6,21].

Fig. 2(b), an enlargement of the portion of Fig. 2(a) where the resolved windows are most abundant, displays the principal findings of this section. Centred near $a = 1.45$, $b = 0.15$ is a dominating window suggestive of a strange creature with a central "body", which we shall call the *centre* of the window, and two narrow "antennae" extending downward to the right and two more extending upward to the right. Within the window, solutions of period 5 or a harmonic are stable; we shall call it a 5-window.

Diagonally below and above the 5-window are somewhat smaller 7-windows, centred near (1.62, 0.08) and (1.24, 0.29). Their shapes are remarkably similar to that of the 5-window, even in their details where these are resolved; with suitable linear changes of coordinates they would nearly superpose on one another. Wherever antennae of two windows intersect, both periods are stable.

Since separate centres are connected by intersecting antennae, one might choose to say that the entire shaded area in Fig. 2(b) constitutes one big window. This is really a matter of definition. To exclude this possibility, let us stipulate that, for a region to qualify as a subwindow, one must be able to travel within the region from any point to any other point by varying a and b continuously, with the accompanying xs also varying continuously, and with the periodicity and its stability preserved. A window is simply a juxtaposition of a fundamental subwindow and its harmonics. Separate centres or their antennae then belong to separate windows.

Many considerably smaller windows, produced by higher periods, line up along the diagonal. Passing through them is a narrow shaded band, and, since only periodic points have been plotted, it must be composed of additional minuscule windows that are detected but not well resolved. We shall call bands of this sort *window streets,* and this particular band the *principal* window street, and, for reasons that will appear in the next

section, we shall call a window with a centre and four or more antennae a *compound window*.

Between the upper 7-window and the 5-window, a 9-window centered near (1.35, 0.26) is clearly off the street. Fig. 3(a), an enlargement of a portion of Fig. 2(b) where the upper 7-window dominates, reveals that above and below the 9-window there are smaller windows that also lie off the street, and that evidently form another street not quite parallel to the first one, extending upward from the lower right corner of the figure. For reasons to appear later we shall regard this street as a branch of the principal street, rather than a separate street. The uppermost antenna from the 9-window, incidentally, passes through (1.4029, 0.3), close to the point (1.4, 0.3) chosen by Hénon for detailed study, although it still misses the point by about 12 antenna widths.

It is interesting to compare a cross-section of Fig. 3(a) along which $b = 0.3$ with graphs of the larger Lyapunov exponent of Eq. (5) against a, presented by Feit [6], Olsen and Degn [20], and Simó [21]. What show up there as a wider and a separate narrower interval of negative values are seen to be the intersections of the line $b = 0.3$ with the body of the 7-window and an antenna of the same window.

Extending upward to the right from the 7-window, between two antennae, is a clearly separate window street, and there are suggestions of other streets. The 7-window exhibits remarkable symmetry about a nearly horizontal line. For good measure we have enlarged, in Fig. 3(b), a small region just above the axis of symmetry of the 7-window and just to the right of the center, 14 times horizontally and 25 times vertically, plotting only points whose periods are multiples of 7, and leaving the lower left corner empty. The result, with a dominating 21-window, is nearly a copy of Figs. 2(b) or 3(a), complete with window streets.

Returning to Fig. 2(b), we note that not all windows are compound. Some of the many parallel bands on the left side are in fact left-hand antennae extending downward from windows centered above them, but at the extreme left they are complete windows by themselves. Of special interest is the 6-window centered somewhat above the 5-window, near (1.51, 0.23), whose uppermost antenna bends back to the left and then widens and makes a loop before heading to the right. The large camel-shaped 8-window near the upper left corner is sui generis.

We must now note that although the Hénon map has been the subject of a multitude of studies, and the numerical indications for chaos are overwhelming, it has yet to be proven that chaos actually occurs with the values $a = 1.4$, $b = 0.3$ chosen by Hénon, or, more importantly, with any pair of values near these [6,9]. Benedicks and Carleson [1] have shown that some points where b is much smaller can produce chaos.

The question thus arises as to the meaning of this entire work, if chaos is in fact not present. Let us note, then, that our definition of a window does not assume that points just outside it are chaotic. It is sufficient that the xs there not be small departures from the xs at points just inside. The concept of a window is therefore not altered.

Two general questions arise. First, why do the compound windows have rather complicated but similar shapes, and what determines these shapes? Second, why do they often line up along rather smooth curves, and what determines these curves? The following sections are aimed at establishing at least partial answers to these questions.

3. Locating the windows by numerical integration

Although random searching can presumably locate any compound window, other procedures are available. Here we shall abandon the "empirical" approach and adopt a "theoretical" one, based on numerical integration along the curves that bound the subwindows. Our approach will be more like the one in [9], but our formulas will refer to general rather than specific windows.

To specify a solution uniquely we need four quantities—the parameters a and b and initial values x_0 and x_1. We assume the mapping to be contracting, so that $|b| < 1$. If one or more quantity is allowed to vary continuously while Eq. (5) remains satisfied,

$$\mathrm{d}x_{n+1} = b\mathrm{d}x_{n-1} - 2x_n\mathrm{d}x_n + \mathrm{d}a + x_{n-1}\mathrm{d}b. \tag{8}$$

If in general

$$\mathrm{d}x_n = P_{n0}\mathrm{d}x_0 + P_{n1}\mathrm{d}x_1 + P_{n2}\mathrm{d}a + P_{n3}\mathrm{d}b, \tag{9}$$

then $P_{ni} = \delta_{ni}$ when $n = 0$ or 1, and, when $n > 0$,

$$P_{n+1,i} = bP_{n-1,i} - 2x_nP_{ni} + \delta_{2i} + x_{n-1}\delta_{3i}. \tag{10}$$

(We separate multiple subscripts by commas when any subscript consists of more than one symbol.)

For variations about a period-K solution, with $x_K = x_0$ and $x_L = x_1$ (for conciseness we write L for $K + 1$), if a and b are held fixed,

$$\begin{pmatrix}\mathrm{d}x_K\\ \mathrm{d}x_L\end{pmatrix} = \begin{pmatrix}P_{K0} & P_{K1}\\ P_{L0} & P_{L1}\end{pmatrix}\begin{pmatrix}\mathrm{d}x_0\\ \mathrm{d}x_1\end{pmatrix}. \tag{11}$$

Since the determinant in Eq. (11) is $(-b)^K$ (K consecutive contractions), the characteristic equation, with roots λ_1 and λ_2 with $|\lambda_1| \geq |\lambda_2|$, is

$$\lambda^2 - (P_{K0} + P_{L1})\lambda + (-b)^K = 0, \tag{12}$$

whence, if we let

$$U = (P_{K0} + P_{L1})/(1 + (-b)^K), \tag{13}$$

$U = \pm 1$ when $\lambda_1 = \pm 1$, the limiting values of λ_1 for stable periodicity. Hence U can serve as a stability measure. Note that U is real, while λ_1 may be complex, and in general $U \neq \lambda_1$, but $|U| < 1$ when $|\lambda_1| < 1$; U is closely related to the quantity Σ in [8]. The boundaries of a compound subwindow should thus be curves along which $U = 1$ or -1. We shall let $\mathrm{d}U = U_0\mathrm{d}x_0 + U_1\mathrm{d}x_1 + U_2\mathrm{d}a + U_3\mathrm{d}b$.

If a and b are allowed to vary while the periodicity is preserved, and while some quantity s determined by the state,

with $ds = s_0 dx_0 + s_1 dx_1 + s_2 da + s_3 db$, is held fixed, and some other quantity t with $dt = t_0 dx_0 + t_1 dx_1 + t_2 da + t_3 db$ varies,

$$\begin{pmatrix} P_{K0}-1 & P_{K1} & P_{K2} & P_{K3} \\ P_{L0} & P_{L1}-1 & P_{L2} & P_{L3} \\ s_0 & s_1 & s_2 & s_3 \\ t_0 & t_1 & t_2 & t_3 \end{pmatrix} \begin{pmatrix} dx_0 \\ dx_1 \\ da \\ db \end{pmatrix} = \begin{pmatrix} 0 \\ 0 \\ 0 \\ dt \end{pmatrix}. \quad (14)$$

Eq. (14) is readily solved for expressions for dx_0/dt, dx_1/dt, da/dt, and db/dt, once s and t have been specified. By treating t as the independent variable we may, given a suitable initial state, integrate these expressions numerically, just as we would if t were time, obtaining a curve along which the periodicity and the value of s are maintained.

In the integrations of greatest interest, $s = U$, so that $ds = dU$. A curve along which periodicity is preserved and U is constant will be called a U-curve. A U-curve with $U = +1$ or -1 will be called a U^+-curve or a U^--curve; such a curve should follow a boundary of a subwindow. Thus, U^+- and U^--curves are fold and flip bifurcation curves, respectively. From Eqs. (8)–(10) it follows that if in general, when $i = 0$ or 1,

$$dP_{ni} = Q_{ni0} dx_0 + Q_{ni1} dx_1 + Q_{ni2} da + Q_{ni3} db \quad (15)$$

then $Q_{nij} = 0$ when $n = 0$ or 1, and

$$Q_{n+1,i,j} = b Q_{n-1,i,j} - 2x_n Q_{nij} - 2P_{ni} P_{nj} - P_{n-1,j} \delta_{3i}, \quad (16)$$

whence, from Eq. (13),

$$U_j = (Q_{K0j} + Q_{L1j} + KU(-b)^{K-1}\delta_{3j})/(1 + (-b)^K). \quad (17)$$

The simplest choice for t would be b, making $t_j = \delta_{3j}$, but if b attains a local extremum on a boundary of the subwindow, the integration will break down; this will be reflected in the vanishing of the determinant of the matrix in Eq. (14). Since in any event the derivatives dx_0/dt, etc., are proportional to the minors of t_0, etc., any choice that prevents the determinant from vanishing (unless all the minors vanish simultaneously) will suffice, and here we simply let t_0, t_1, t_2, t_3 be multiples of their respective minors.

A convenient initial state on a U-curve is its intersection with the line $b = 0$. When $b = 0$ and only then, Eq. (5) reduces to the first-order two-to-one mapping

$$x_{n+1} = a - x_n^2, \quad (18)$$

a form of the logistic equation, obtainable from Eq. (2) by letting $a = (\alpha - 2)\alpha/4$ and $x_n = (2X_n - 1)\alpha/2$. We shall call the line $b = 0$ the *logistic* line, or simply the b-line, and the windows on this line *logistic* windows, or b-windows.

Each compound Hénon-window has two antennae extending downward or upward across the b-line, and the short segments in which they intersect it are b-windows; thus each compound window is associated with two distinct b-windows. As already mentioned, these windows have been intensively studied, and here we shall simply note a special procedure for locating them, which involves integrating numerically along the b-line with $a = 2$ initially, while preserving periodicity.

On this line, if $n > 0$, $P_{n0} = 0$, so that $U = P_{L1}$, while the first and last terms on the right of Eq. (9) drop out. A sufficient condition for periodicity is now $x_L = x_1$, whence $dx_L = dx_1$. It follows that we can integrate the equation

$$dx_1/da = -P_{L2}/(U - 1) \quad (19)$$

numerically (until U reaches 1), and thus, given x_1 when $a = 2$, determine the values of x_1 and U, and hence of all the xs, when a reaches any particular value. If $|U| < 1$, a lies in a b-subwindow.

A more convenient alternative is to choose U as the variable of integration ($t = U$), making it easy to carry the computation to a prechosen value of U. Since $U = P_{L1}$, $t_j = Q_{L1j}$, so if periodicity is preserved

$$\begin{pmatrix} P_{L1}-1 & P_{L2} \\ Q_{L11} & Q_{L12} \end{pmatrix} \begin{pmatrix} dx_1 \\ da \end{pmatrix} = \begin{pmatrix} 0 \\ dU \end{pmatrix}, \quad (20)$$

from which expressions for dx_1/dU and da/dU are readily obtained.

As often noted [6,12], when $a = 2$ the general solution of Eq. (18) may be expressed explicitly, since, if $x_0 = -2\cos\theta_0$ for some θ_0, $x_1 = -2\cos(2\theta_0)$ and more generally $x_n = -2\cos(2^n\theta_0)$. If $|x_0| > 2$ so that no real θ_0 exists, the solution is one that blows up.

It follows that for a solution of period K, $\cos(2^K\theta_0) = \cos\theta_0$, so that $\theta_0 = j\phi_K$, for some integer j, where $\phi_K = \phi'_K = 2\pi/(2^K + 1)$ or $\phi_K = \phi''_K = 2\pi/(2^K - 1)$. Consider the former alternative. If, for any n, i_n is the smallest nonnegative integer that makes $\cos(i_n\phi'_K) = \cos(2^n\theta_0)$, we find that $i_{n+1} = 2i_n$ or $2^K + 1 - 2i_n$. It is convenient to number the xs so that x_0 is the x closest to 0, whence x_1 and x_2 are the extreme positive and negative xs, respectively, and i_1 and i_2 are the largest and smallest integers in the sequence of is. We shall refer to the particular period-K solution where $i_2 = j$ as period $K(j)$. Note that period $K(j)$ does not exist when j exceeds some other integer in the sequence.

Since, for such a solution, U is just $(-2)^K$ times the product of the xs, U is 2^{2K} times a product of cosines. Since also $\cos\theta\cos 2\theta = (\cos\theta + \cos 3\theta)/2$, and hence $\cos\theta\cos 2\theta\cos 4\theta = (\cos\theta + \cos 3\theta + \cos 5\theta + \cos 7\theta)/4$, etc., we find that $U = -2^K$ if $\phi_K = \phi'_K$ while $U = 2^K$ if $\phi_K = \phi''_K$.

We can now perform the integration along the b-line, once K and j are specified. We shall extend the definition of $K(j)$ to the periodic solutions obtainable by such an integration from a solution where $a = 2$, and also to the b-windows containing the solutions, and to certain curves extending from these b-windows. The 7-window in Fig. 3(a) proves to intersect the 7 (11) and 7 (21) b-windows.

Table 1 shows values of a and x_n for selected values of U, including -1, 0, and 1, as determined by numerical integration with U as the independent variable, with a fourth-order Runge–Kutta scheme with an increment of 1.0, for periods 7(11) and 7(21). In either case $U = -128$ initially, and the integration is continued until $U = 128$. We see that a, after reaching a minimum when $U = 1$, returns to 2 at the end, and, in fact, the accompanying values of x_n are precisely the cosine solution that would have been used initially with $\phi_K = \phi''_K$. The narrow ranges of a where $|U| < 1$ are seen to fit within the intersections of antennae of the 7-window with the b-line in

Fig. 2(b). A similar procedure can in principle be used to locate any desired subwindow.

Having found the points on the b-line where U assumes specified values, we can perform numerical integrations along the U-curves. From Table 1 we see that the 7(21) U^+- and U^--curves must be close together when $b = 0$, but they diverge as b increases. One might have supposed that the U-curves with $|U| < 1$, which contain all the points where period 7 is stable, would fill the space between the U^+- and the U^--curve, but Fig. 4(a), showing portions of the U-curves near the center at intervals of 1/4 unit, reveals that this is not the case. One set of curves continues upward, following the U^+-curve, while another set turns to the right, following the U^--curve. No curves enter the upper right region. Separating the sets is a single U-curve (not shown) with $U = 0.0064$, terminating at a singular point where $a = 1.235$, $b = 0.296$, shown as a dot. Fig. 4(b) shows similar curves originating in the 7(11) subwindow. The U^+-curve possesses a cusp, about which the nearby U-curves loop. Again no curves enter the upper right region, and a separating curve terminates at the same singular point.

The Runge–Kutta scheme can give inadequate and sometimes bizarre results if the time increment is too large. An increment that is suitable on one part of a curve may be too long on another. Particularly with our procedure for defining $\mathrm{d}t$, it is not obvious in advance what increment is appropriate. We have, therefore, for selected U-curves, performed several integrations with successively smaller increments, until further reduction by a factor of two produces no difference in the 5-decimal-place output.

At a cusp on a U-curve, $\mathrm{d}a/\mathrm{d}x_0$ and $\mathrm{d}b/\mathrm{d}x_0$ vanish as x_0 varies along the curve. Returning to Eq. (14) with $s = U$ but with $t = x_0$, so that $t_j = \delta_{0j}$, numbering the rows and columns of the matrix from 0 to 3 and letting C_{ij} be the determinant of the elements in rows 0 and 1 and columns i and j, while D_{ijk} is the determinant of those in rows 1, 2, 3 and columns i, j, k, we find that $\mathrm{d}a/\mathrm{d}x_0 = D_{013}/D_{123}$ and $\mathrm{d}a/\mathrm{d}x_1 = -D_{012}/D_{123}$. After some algebra we find that $C_{12}\mathrm{d}a/\mathrm{d}x_0 + C_{13}\mathrm{d}b/\mathrm{d}x_0 = C_{01}$. According to Eq. (12), vanishing of C_{01} implies that $\lambda_1 = 1$, so that $U = 1$, whence any cusp on a U-curve must lie on a U^+-curve.

Fig. 4(c) simply superposes Fig. 4(a) and (b). There is a symmetry about the line that passes through the cusp and the singular point, not obvious in Fig. 4(a) and (b) separately, and, contrary to what occurs in these figures, the U-curves with $|U| < 1$ fill the space bounded by the U^+- and U^--curves.

Fig. 4(d) has been produced by random searching, exactly in the manner of Fig. 2, except that only those points where $K = 7$ are plotted. No harmonics are included. It thereby shows a period-7 principal subwindow, which is somewhat simpler in shape than a complete compound window, but still has a center and four antennae. We see that it fits exactly onto the region covered by the curves in Fig. 4(c).

The U^+- and U^--curves originating in the two b-windows have not simply happened to encounter each other temporarily; they have effectively switched partners. Each U^--curve closely follows the course of a U^+-curve, forming one antenna, until it nears the centre, but it then crosses the other U^--curve, and upon receding from the centre it is seen to be accompanying the other U^+-curve, forming another antenna. In view of this behaviour the term "compound window" seems appropriate.

Similarly constructed U^+-curves for the 5-window agree with the bounding curves of Hitzl and Zele [9], who note the cusp. Their figure covers a wide range of a, however, making it difficult to distinguish the U^-- from the U^+-curves, and the divergence of the former from the latter as they approach or recede from the cusp, which gives the centre of the subwindow its characteristic shape, is not revealed.

The shape does appear prominently in an extensive study by Mira [17] of bifurcations in mappings, with the Hénon map as a specific example. One should compare the U^+- and U^--curves in our Fig. 4 with his Fig. 6.27, where he displays the fold and flip bifurcation curves near the centres of the 5-, 6-, and two 7-windows that appear in our Fig. 2(b).

Mira has identified three special types of area within parameter space – the crossroad, spring and saddle areas – characterized by different relative locations of the bifurcation curves. In Fig. 6.28 he shows the peculiar 8-window, which, like the windows in Fig. 6.27, belongs in a crossroad area, but involves a three-way rotation of partners, while in Fig. 6.32 he deals with the upper loop of the 6-window, which belongs in a spring area. In subsequent works [2,18,19], he and his coworkers investigate the transitions among the areas, and they present a "skeleton" of a crossroad area, with the now familiar shape of our Fig. 4(c) and (d).

4. A generic compound window

If a typical window had been bounded by a simple curve, perhaps an ellipse, we might never have been led to ask why. The more complicated actual boundary, which has raised questions, or at least the boundary of an idealized compound window, nevertheless yields to a reasonably simple mathematical formula.

We note first that when $b \neq 0$, vanishing of x_0 does not assure us that $U = 0$, but, particularly when b is small, a large x_0 favours a large U. When $K = 5$, for example,

$$(1 - b^5)U = -32x_0x_1x_2x_3x_4 - 8b\sum_{n=0}^{4} x_nx_{n+1}x_{n+2} - 2b^2\sum_{n=0}^{4} x_n. \tag{21}$$

When K assumes other values, the leading term in a similar expression is also $(-2)^K$ times the product of the xs. If x_0, the smallest x, is not small, it is unlikely that the later terms on the right can nearly cancel the dominant leading term.

Table 1, which is typical, has indicated that, with $b = 0$, x_0 remains small enough to make $|U| < 1$ only through narrow ranges of a—the logistic subwindows. Near the centre of a compound window the range of a, and so very likely the extreme value of $|x_0|$, is considerably larger. It is nevertheless

Table 1
Values of a and $x_0, \ldots, x_6$ corresponding to selected values of U in period-preserving numerical integrations along the b-line

U	a	x_0	x_1	x_2	x_3	x_4	x_5	x_6
Period 7(11)								
−128.0	2.00000	0.267	1.929	−1.720	−0.958	1.083	0.827	1.316
−96.0	1.96026	0.215	1.914	−1.703	−0.940	1.077	0.800	1.321
−64.0	1.92383	0.154	1.900	−1.687	0.922	1.074	0.770	1.330
−32.0	1.89608	0.081	1.889	−1.674	−0.906	1.075	0.741	1.347
−1.0	1.88484	0.003	1.885	−1.668	−0.897	1.081	0.716	1.372
0.0	1.88480	0.000	1.885	−1.668	−0.896	1.081	0.715	1.373
1.0	1.88479	−0.003	1.885	−1.668	−0.896	1.082	0.715	1.374
32.0	1.89501	−0.082	1.888	−1.670	−0.895	1.094	0.699	1.406
64.0	1.92288	−0.157	1.898	−1.681	−0.902	1.109	0.693	1.442
96.0	1.95995	−0.219	1.912	−1.695	−0.914	1.124	0.696	1.476
128.0	2.00000	−0.271	1.926	−1.711	−0.928	1.139	0.702	1.507
Period 7(21)								
−128.0	2.00000	−0.506	1.744	−1.042	0.914	1.164	0.646	1.583
−96.0	1.91743	−0.452	1.713	−1.018	0.881	1.141	0.615	1.539
−64.0	1.81693	−0.377	1.675	−0.989	0.839	1.112	0.580	1.481
−32.0	1.68908	−0.254	1.625	−0.950	0.787	1.070	0.543	1.394
−1.0	1.57541	−0.010	1.575	−0.906	0.754	1.007	0.562	1.259
0.0	1.57489	0.000	1.575	−0.905	0.755	1.005	0.566	1.255
1.0	1.57472	0.010	1.575	−0.905	0.756	1.003	0.569	1.251
32.0	1.67251	0.250	1.610	−0.920	0.826	0.990	0.693	1.193
64.0	1.80223	0.376	1.661	−0.955	0.889	1.011	0.780	1.194
96.0	1.90981	0.456	1.702	−0.987	0.935	1.035	0.839	1.206
128.0	2.00000	0.514	1.736	−1.014	0.971	1.057	0.884	1.219

possible for U to remain small if, as x_0 becomes only moderately small, some other x, say x_m, becomes rather small.

A major difference between the two integrations displayed in Table 1 is the sign of x_3. If in Fig. 4(c) one travels along U-curves from one b-window to the singular point and then to the other b-window, x_3 must have a zero crossing somewhere, allowing U to remain small. This is also true for the 5-window.

It may therefore be enlightening to view the curves of Fig. 4 in a new system with x_0 and x_m as coordinates. Note that Eq. (21), and similar equations for other values of K, may be rewritten as

$$U = B_{0m}x_0x_m + B_0x_0 + B_mx_m + B. \tag{22}$$

The coefficients, functions of b and the remaining xs, are not constants, but, in the case of Eq. (21) with $m = 3$, for fairly extensive variations of x_0 and x_3 about 0, they do not change sign, and are relatively constant, so we may expect the new U-curves to look somewhat like rectangular hyperbolas with common asymptotes. Fig. 5 shows the new curves, for $U = 1$, 0, and -1. The hyperbolic appearance is confirmed.

Consider next either an extremum or a saddle point of a, where $\partial a/\partial x_0$ and $\partial a/\partial x_m$ vanish. Letting $s = x_m$ and $t = x_0$ in Eq. (14), so that $s_j = P_{mj}$ and $t_j = \delta_{0j}$, we find that $\partial a/\partial x_0 = D_{013}/D_{123}$ and $\partial a/\partial x_m = -C_{13}D_{123}$. Again after some algebra we find that $C_{12}\partial a/\partial x_0 + D_{012}\partial a/\partial x_m = C_{01}$. As with the cusp, the point, and a similar point for b, must lie on a U^+-curve.

Without a formal treatment we note, say from Fig. 4(a), that near the center of a typical compound window a has an absolute minimum – U-curves with $U < 1$ or $U > 1$ lie to the right of the U^+-curve – while b lacks a minimum and at most has a saddle point. Accordingly, we shall construct a "generic" compound window by first letting $U = x_0x_m$, and then letting the lines of constant a be concentric circles centered at (1, 1), and those of constant b be rectangular hyperbolas with common asymptotes, centred at $(-1, -1)$, points where $U = 1$. The simplest choice is $a = (x_0 - 1)^2 + (x_m - 1)^2$, $b = (x_0 + 1)^2 - (x_m + 1)^2$. Eliminating x_0 and x_m yields the fourth-degree equation

$$(b^2 - a^2 - 20a + 12 - 8U + 4U^2)^2 - (8a + 16 - 8U)^2(a - 1 + 2U) = 0. \tag{23}$$

With U specified, the values of b corresponding to any chosen a are easily found, and b may be plotted against a.

Fig. 6 superposes such plots for selected values of U. We have effectively reproduced Fig. 4(c). The typical shape of a compound subwindow, although not rigorously derived, is at least shown to be one that is not unreasonable. Polynomial expressions have previously been noted [2] for bifurcation surfaces in a first-order three-parameter map. Of course, in the formulas for the actual U-curves, the fourth-degree terms are at most the dominating ones. A similar although more involved analysis could perhaps "explain" the typical structure of a complete compound window, with its harmonics.

5. The principal window street

The visible branches of the principal window street in Figs. 2 and 3 are suggestive of smooth curves, but, since they are composed of portions of windows, they must have finite

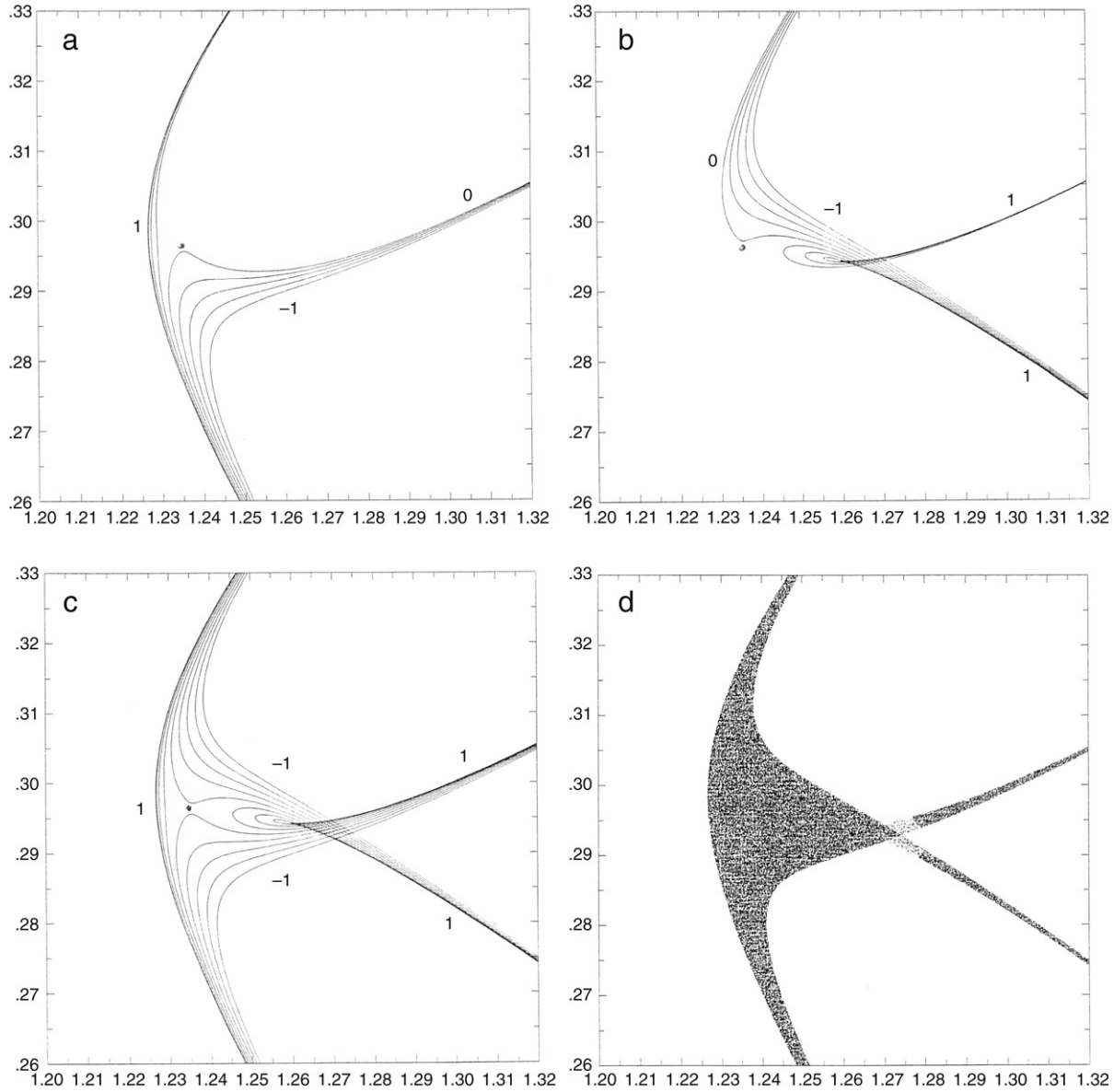

Fig. 4. (a) Portions of U-curves from $U = 1$ to $U = -1$, at intervals of 1/4, that extend from 7(21) logistic subwindow. (b) The same as Fig. 4(a), but extending from 7(11) logistic subwindow. (c) Superposition of Fig. 3(a) and (b). (d) Portion (shaded) of area covered by Fig. 3(a)–(c) where period 7 is stable, as determined by random searching. Horizontal scales indicate a, vertical scales indicate b, numbers beside curves indicate U.

widths. In this section we shall establish a procedure for closely approximating them by readily defined smooth curves. Such a curve might pass through some special point of each window along a branch.

Obvious special points of a compound window are the cusp on the right-hand U^+-curve and the singular point, but another point, to be called the 0-3 point, proves to be more convenient. We shall first demonstrate that the street is closely approximated by the set of 0-3 points, which we shall in turn approximate by definable curves.

We have hypothesized that in the central portion of each compound window, two xs in the stable periodic solution are small. We have discovered that in the 5-window and two 7-windows one small x follows the other by three iterations. It therefore seems possible that within each of these windows, and also within or close to a typical window on the principal street, one pair of values (a, b) produces a periodic solution with $x_0 = x_3 = 0$. Such a pair, when it exists, is readily located by identifying a suitable logistic window, locating the point in it where $x_0 = 0$, and then integrating numerically, while preserving the periodicity and holding x_0 fixed, until $x_3 = 0$. We shall call a curve produced in this manner a 0-curve, and the point on it where $x_3 = 0$ a 0-3 point. Not all 0-curves reach 0-3 points.

Fig. 7(a) contains the 0-curves extending from the 7(11) and 7(21) logistic windows—the windows from which the U-curves in Fig. 4 extend. The 0-curves meet at a common 0-3 point, indicated by the arrow. Together they form such a smooth curve that the 0 3-point looks no different from any other point, and if either integration were carried past the 0-3-point it would produce the other 0-curve.

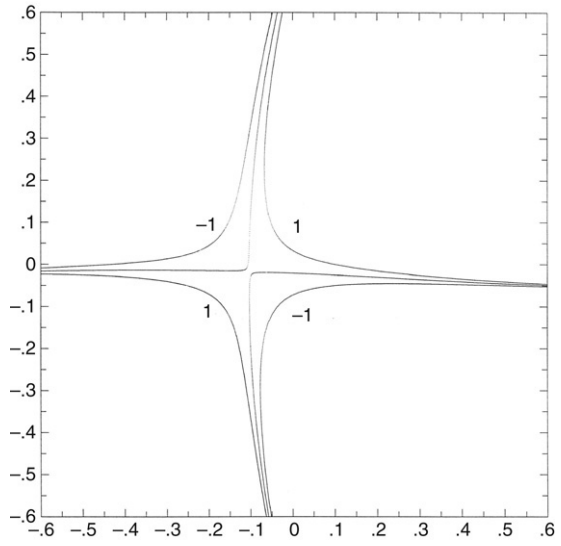

Fig. 5. The curves of Fig. 4(c) where $U = 1$, 0, and -1, in a transformed coordinate system. Horizontal scale indicates x_0, vertical scale indicates x_3, numbers beside curves indicate U.

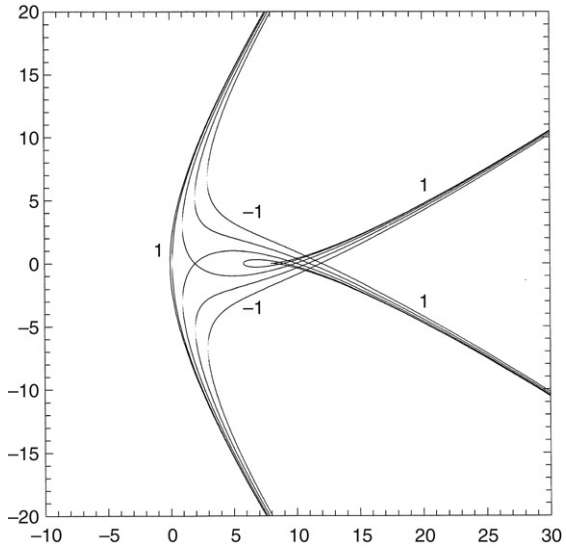

Fig. 6. Segments of generic U-curves from $U = 1$ to $U = -1$, at intervals of $1/2$. Horizontal scale indicates a, vertical scale indicates b, numbers beside curves indicate U.

Fig. 7(b) superposes the 0-curves extending from all $K(j)b$-windows where $K \leq 11$, and where $2^K/12 < j < 2^K/6$ and $j = 3$ or 5 (mod 8), for which the integration can be carried to the 0-3 point. When j is smaller or larger the curves tend to be rather far to the right or left of the principal street, while the restriction (mod 8) eliminates cases where $b < 0$ at the 0-3 point. Every 0-curve joins another one to form as smooth a combined curve as in Fig. 7(a). Each combined curve is quasi-parabolic, and the axes of the parabolas seem to follow one or the other of the two branches of the street. Moreover, examination reveals that whenever two curves join, say the curves from the $K(j)$ and $K(j')$ windows, $j + j' = 2^K/4$.

When instead $j = 1$ or 7 (mod 8), the x that eventually vanishes as one travels along a 0-curve precedes rather than follows x_0 by three iterations, so that $x_0 = x_{K-3} = 0$. In all cases that we have examined, $j - j' = 2$.

It seems reasonable that the U^+- and U^--curves extending from two windows that share a 0-3 point should meet to form the boundaries of a compound subwindow, with which the 0-3 point may be associated. This certainly happens when $K = 5$ or 7, but a general conclusion does not follow.

Fig. 8 shows 0-3 points with $b > 0$ for $K \leq 24$, and those with $b < 0$, which crowd more closely together, for $K \leq 18$. As might have been expected from Fig. 7(b), the points seem to lie on a complex of curves rather than a single curve. The curves visibly separate when b is low, and again when b is higher. The second separation is easily seen in the tenfold enlargement of the uppermost points of the right-hand branch, produced with

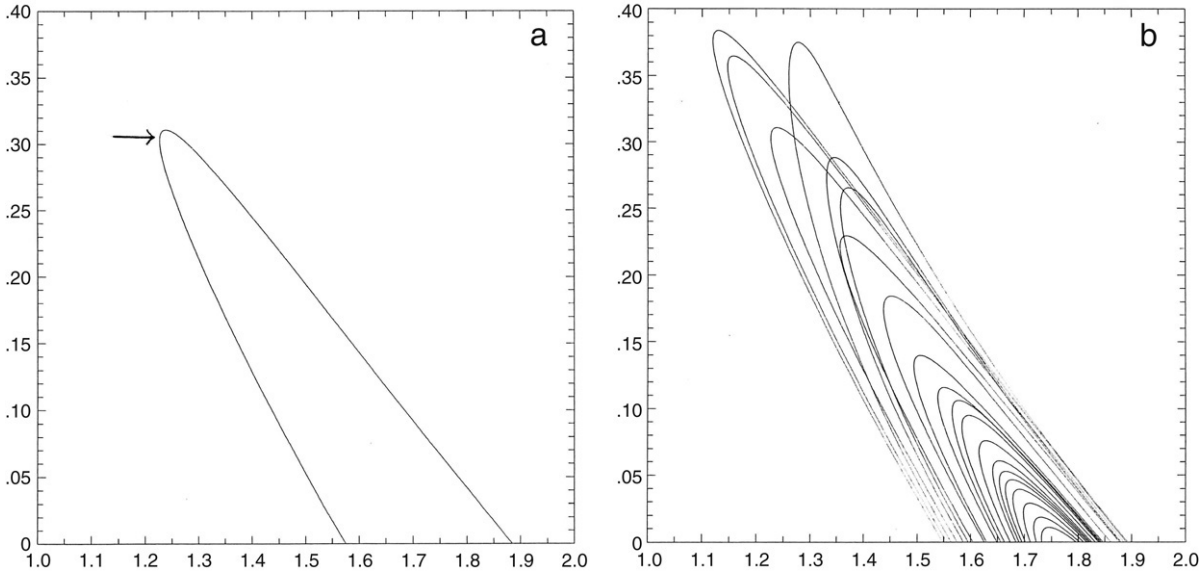

Fig. 7. (a) The 0-curves extending from the 7(21) and 7(11) logistic windows, meeting at 0-3 point indicated by arrow. (b) The 0-curves extending from all $K(j)$ windows with $K \leq 11$ and $2^K/12 < j < 2^K/6$ and $j = 3$ or 5 (mod 8), meeting in pairs at 0-3 points (not shown). Horizontal scales indicate a, vertical scales indicate b.

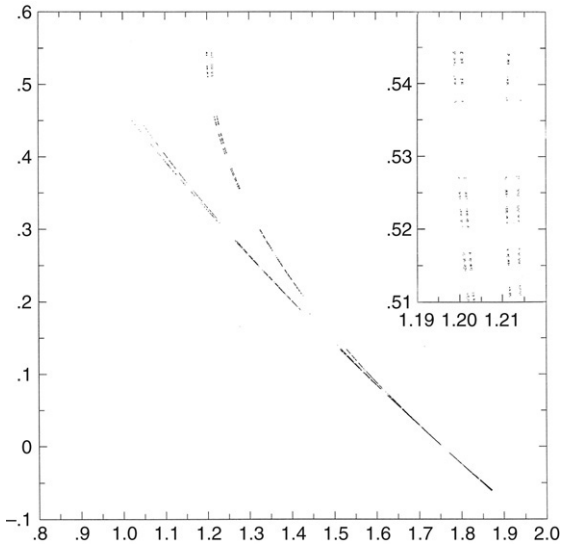

Fig. 8. The 0-3 points that terminate the 0-curves from all $K(j)$ logistic subwindows with $2^K/12 < j < 2^K/6$, and with $K \leq 24$ when $j = 3$ or 5 (mod 8) and $K \leq 18$ when $j = 1$ or 7 (mod 8). Inset in upper right is tenfold enlargement of points where $b > 0.51$ that terminate 0-curves from logistic subwindows with $2^K/12 < j < 2^K/6$ and $K \leq 30$. Horizontal scales indicate a, vertical scales indicate b.

$K \leq 30$, and a third separation appears. It seems likely that if enough points could be plotted, they would be seen to lie on a Cantor set of curves. The left-hand branch passes through or near most of the windows of Fig. 2(b) and Fig. 3(a), but the prominent 9-window lies on the right-hand branch.

Although the 0-3 points may lie along smooth curves, they do not fill such curves, since they are defined only for periodic solutions. We shall seek a procedure for defining continuous curves that approximate the curves along which the 0-3 points appear to lie.

Such curves presumably must pass through chaotic as well as periodic points. Except when $b = 0$, a continuum of values of a can produce solutions where $x_0 = x_3 = 0$. We need a condition that chooses among these values where chaos prevails, and that selects a 0-3 point or one close to it where periodicity prevails.

One condition satisfied by all periodic solutions and some but not most chaotic solutions is that the solution does not blow up when iterated backward. Among such solutions are those that originate on the unstable manifold of a steady or periodic solution. Let us examine those on the unstable manifold of the fixed point x^*, the positive root of $x^{*2} + (1-b)x^* - a = 0$. On this manifold successive values of $x_n - x^*$ increase by the factor λ, the negative root of $\lambda^2 + 2x^*\lambda - b = 0$.

Fig. 9(a) shows a plot of x_3 against x_0 along the manifold, for $a = 1.08$ and $b = 0.38$. The point (0, 0), represented by the central dot, lies below and slightly to the right of several local minima of x_3. Fig. 9(b) is similarly produced, but with $a = 1.28$. The manifold has stretched out considerably as a has increased, and more local minima of x_3 are resolved—presumably they form a Cantor set – and now the point (0,0) lies to the left of the curves that extend downward through the minima. By continuity there should be some easily resolvable values of a somewhat above 1.08, and some others somewhat below 1.28, that make the manifold pass through (0,0), i.e. that make the solution with $x_0 = x_3 = 0$ approach x^* instead of $-\infty$ as $n \to -\infty$.

Ideally, given b, we might seek the entire Cantor set of values of a that place the point $x_0 = x_3 = 0$ on the unstable manifold, but we shall instead seek a finite number of values, each of which is close to one or another member of the Cantor set. On the unstable manifold $x_n - x^* \to 0$ as $n \to -\infty$, while $(x_n - x^*) - \lambda(x_{n-1} - x^*) \to 0$ even more rapidly, so we may accomplish our aim by letting one of these quantities vanish for some finite negative value of n. It proves convenient to let

$$F_n = -b\left((x_n - x^*) - \lambda(x_{n-1} - x^*)\right)/\lambda. \tag{24}$$

Substituting $(x_{n+1} - x^*) + (x_n^2 - x^{*2})$ for $b(x_{n-1} - x^*)$, and then substituting $\lambda^2 + 2\lambda x^*$ for b, we obtain

$$F_n = (x_{n+1} - x^*) - (\lambda - x_n + x^*)(x_n - x^*). \tag{25}$$

It appears that we can obtain reasonable results with $n = -2$; i.e. by letting our condition be $F_{-2} = 0$. Given b, it is convenient to choose a succession of values of x_1 rather than a, and then evaluate in turn $x_2, a, x_{-1}, x_{-2}, x^*, \lambda$, and F_{-2}. When $b = 0$ the procedure breaks down, but it also becomes unnecessary, since the Cantor set degenerates to the single value $a = c^2 = 1.7549$, where $c = 1.3247$ is the real root of the equation $x^3 - x - 1 = 0$. Fig. 10 shows curves of F_{-2} against a for selected values of b. The curves are quasi-parabolic with small negative minima. Note that the minima are displaced leftward and the zero crossings become farther apart as b increases.

In Fig. 11 the zero crossings from Fig. 10 and for other values of b are joined to form two curves—the desired curves where $F_{-2} = 0$. Superposed on them are the 0-3 points from Fig. 8. The fit is seen to be good even if not perfect.

It is also possible to produce either curve of Fig. 11 by numerical integration, starting on the logistic line, with the constraints that $\mathrm{d}x_0 = 0$, $\mathrm{d}x_3 = 0$, and $\mathrm{d}F_{-2} = 0$. At the start $a = c^2$, $x_1 = c^2$, and $x_2 = -c$, and x_{-1} must equal x_2 or $-x_2$. The condition $\mathrm{d}x_3 = 0$ becomes $-4c^3\mathrm{d}x_1 + (2c+1)\mathrm{d}a + c^2\mathrm{d}b = 0$, and, with $x_0 = 0$, the condition $\mathrm{d}x_1 = \mathrm{d}(bx_{-1} - x_0^2 + a)$ becomes $-\mathrm{d}x_1 + \mathrm{d}a + x_{-1}\mathrm{d}b = 0$. Thus, with $x_{-1} = -c$, $\mathrm{d}a/\mathrm{d}b = (5c^2 + 4c)/(2c + 3) = 2.491$, while, if $x_{-1} = c$, $\mathrm{d}a/\mathrm{d}b = -(3c^2 + 4c)/(2c + 3) = -1.870$. The former choice makes the curve leave the b-line with a positive slope and follow the curve where $x_0 = 0$ within the period-3 window, so clearly the latter choice, $x_{-1} = -x_2 = c$, is needed to follow the window street. In this case $x_{-2} = \pm\sqrt{c^2 - c}$; either sign is allowable. Integrations with $x_{-2} > 0$ and $x_{-2} < 0$ will produce the left-hand and right-hand curves in Fig. 11, respectively. Consistently with this finding, if in constructing Fig. 8 we had plotted only those points that produce solutions with $x_{K-2} > 0$, only the left-hand branch would have appeared; with $x_{K-2} < 0$, only the right-hand branch appears.

The condition $F_{-2} = 0$ thus appears acceptable. We shall call a curve produced in this manner a *street curve,* and the particular curves, where the vanishing xs in the solutions

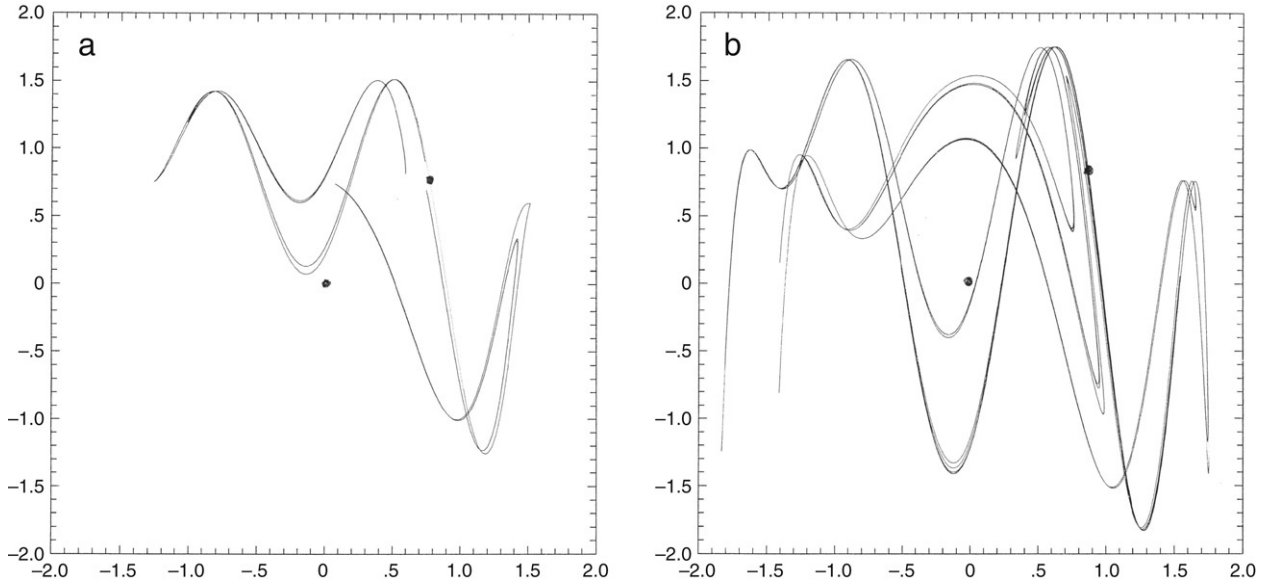

Fig. 9. (a) Unstable manifold of fixed point (x^*, x^*) when $a = 1.08$ and $b = 0.38$, in system with x_0 and x_3 as coordinates. Dot in centre is $(0, 0)$; dot on manifold is (x^*, x^*). (b) The same as Fig. 9(a), but when $a = 1.28$ and $b = 0.38$. Horizontal scale indicates x_0, vertical scale indicates x_3.

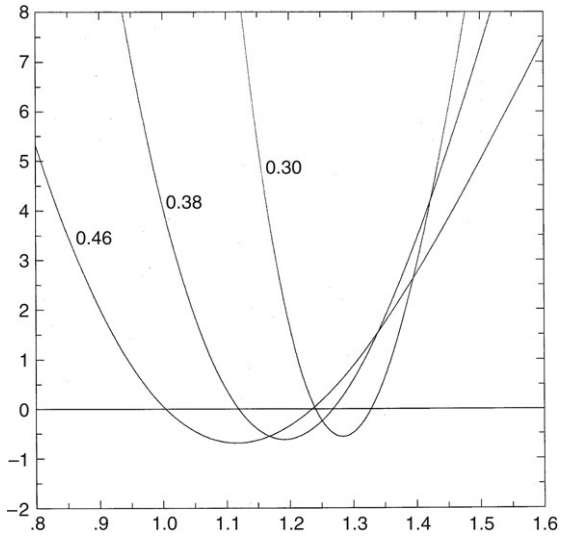

Fig. 10. Curves of F_{-2} against a, for $b = 0.30, 0.38$, and 0.46. Numbers beside curves indicate values of b. Horizontal scale indicates a, vertical scale indicates b.

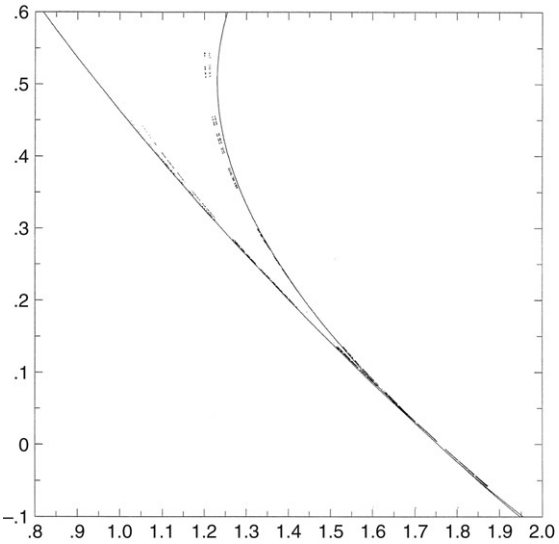

Fig. 11. Branches of street curve of order 3, as determined by numerical integrations starting on logistic line, with 0-3-points from Fig. 8 superposed. Horizontal scale indicates a, vertical scale indicates b.

are three iterations apart, street curves of *order* three. To approximate more members of the Cantor set by street curves we would have to replace the condition $F_{-2} = 0$ by $F_n = 0$ with $n < -2$, and use various choices for the signs of x_{-2}, x_{-3}, etc.

6. Intersecting window streets

Consider the prominent 7-windows in Fig. 2(b), one of which is enlarged in Fig. 3(a). Each one lies on the principal street, and each appears to lie also at the lower end of another street extending to the right. If a period-7 solution has two zeros three iterations apart, it necessarily has two zeros four iterations apart. That is, a 0-3 point associated with a period-7 solution should also qualify as a 0-4-point, and the set of 0-4 points should lie on a complex of curves somewhat like the one implied in Fig. 8. More generally, there should be 0-m points, lying on 0-curves that presumably extend from b-windows other than those associated with 0-3 points, and are obtainable like the 0-3 points, but with $x_0 = x_m = 0$ or $x_0 = x_{K-m} = 0$.

Like the points in Fig. 8, a set of 0-m points may be approximated by a street curve of order m, obtainable like the curves in Fig. 11 by numerical integration, but starting at a b-window of period m. Fig. 12 shows such curves for $2 \le m \le 6$. In each case the third condition has been $F_{-2} = 0$, and initially $x_{-1} = -x_{K-1}$ and $x_{-2} > 0$. Additional curves could be obtained with $x_{-2} < 0$.

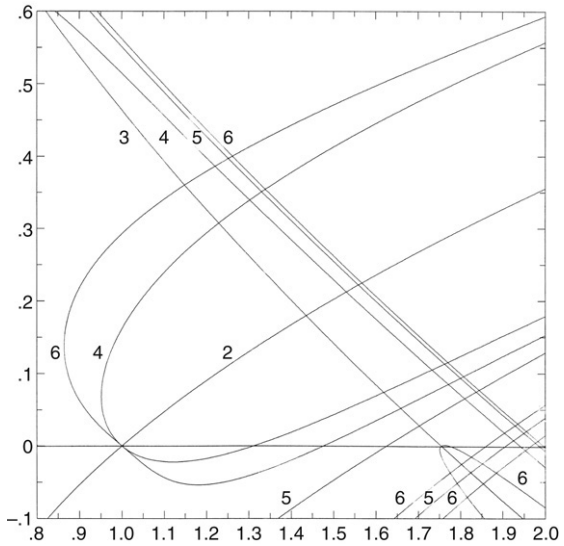

Fig. 12. Street curves of orders $m \leq 6$ as determined by numerical integrations starting on logistic line, with $x_{-2} > 0$. Horizontal scale indicates a, vertical scale indicates b, numbers beside curves indicate m.

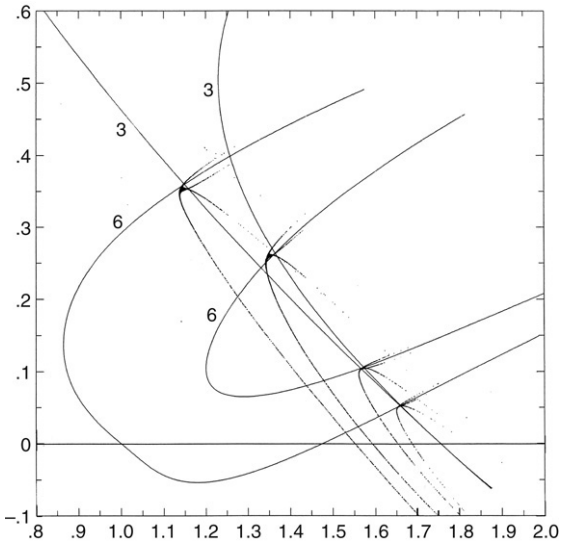

Fig. 13. Selected street curves of orders $m = 3$ and $m = 6$ as determined by numerical integrations starting near centres of 9-windows, superposed on 9-windows as determined by random searching. Horizontal scale indicates a, vertical scale indicates b, numbers beside curves indicate m.

Comparison with Fig. 2(b) shows that the centres of the compound windows of lowest period – the 5-window and the two 7-windows on the principal street and the 6-window to the right – all lie close to intersections of two street curves, the sum of whose orders is the period. We are led to the hypotheses that every compound window is centred on or near an intersection of two street curves. Note that some of the street curves have extensive portions where no corresponding streets appear in Fig. 2(b). This should be expected if streets, which consist of windows, are confined to regions near where street curves intersect.

Further comparison fails to reveal an expected street curve of order 6 passing near the centre of the 9-window on the right-hand branch of the principal street, prominent in figure Fig. 3(a). This is true also of the less prominent 9-window above the lower 7-window. If our hypothesis is correct, there must be additional street curves that do not intersect the logistic line. These, if they exist, as well as the street curves already produced, may be found by integrations originating near already detected 0-m-points.

Fig. 13 contains the four 9-windows on the principal street, as found by random searching, and superposed on these are two street curves of order 6 obtained by integrations starting near the 0-6-points that are near the centres of the upper two 9-windows. Each of these passes near the center of one of the lower 9-windows, and one curve is found not to intersect the b-line. Also included in the figure are street curves of order three obtained by integrations starting near the upper 9-windows. The curves found in this manner are indistinguishable from those in Fig. 11.

The locations of the shorter-period compound windows are thus reasonably well accounted for. When the period is higher, it seems possible that stability might be favoured by having three or more small xs, which could happen if three or more window streets come close to having a common intersection.

7. Further considerations and conclusions

Throughout this work our conclusions regarding the properties of compound windows have been drawn primarily from the study of particular cases. We have not offered mathematical proofs of propositions that the encountered properties are completely general. There is a good reason for this; such propositions tend not to be true.

Consider, for example, the proposition that if period $K(j)$ exists, with $2^K/8 < j < 2^K/6$ and $j = 3$ or 5 (mod 8), then period $K(j')$ where $j + j' = 2^K/4$ exists (whence $2^K/12 < j' < 2^K/8$ and $j < 2j'$), and the $K(j)$ and $K(j')$ 0-curves meet at a common 0-3-point. Consider also the proposition that, under the same conditions, as b increases, the U^--curve extending from either logistic subwindow diverges from the U^+-curve extending from the same subwindow, crosses the other U^--curve and nears the other U^+-curve, so that the curves together form boundaries of a compound subwindow, with four antennae.

We have found no exceptions to the first proposition among the 272 cases where $K \leq 17$. The second proposition fails in one of the 20 cases where $K = 13$.

Fig. 14(a) shows segments of the 13(1363) and 13(685) U^+- and U^--curves. The U^+-curves appear normal, with a cusp on the right-hand curve, but the U^--curves fail to cross. U-curves with $U = -1.343$ from either b-window meet at a common singular point, outside the region of stability. Fig. 14(b), obtained by random searching, confirms that there are two separate period-13 windows.

A figure showing several U-curves with U ranging from 1 to -3 rather than 1 to -1 would resemble Fig. 4(c), but the region covered by the curves would no longer be a subwindow. We shall call a pair of windows produced in the manner of Fig. 14 an *almost-compound* pair.

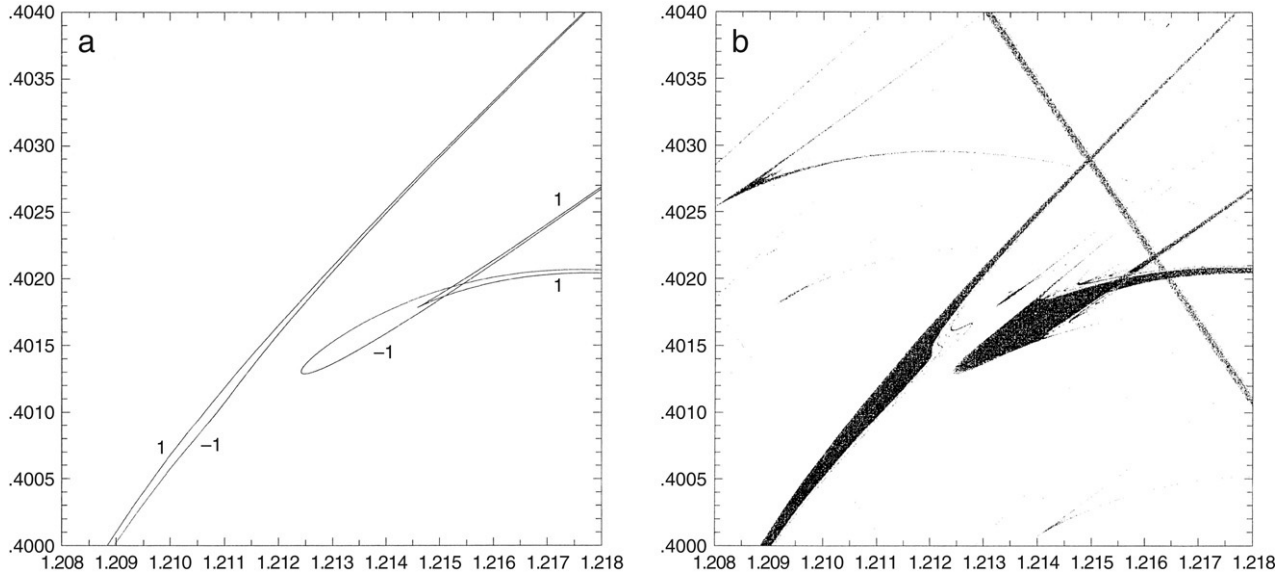

Fig. 14. (a) Portions of U^+ and U^- curves that extend from 13(1363) and 13(685) logistic subwindows. (b) Portion (shaded) of area covered by Fig. 14(a) where stable periodic solutions occur, as determined by random searching. Horizontal scales indicate a, vertical scales indicate b, numbers beside curves indicate U.

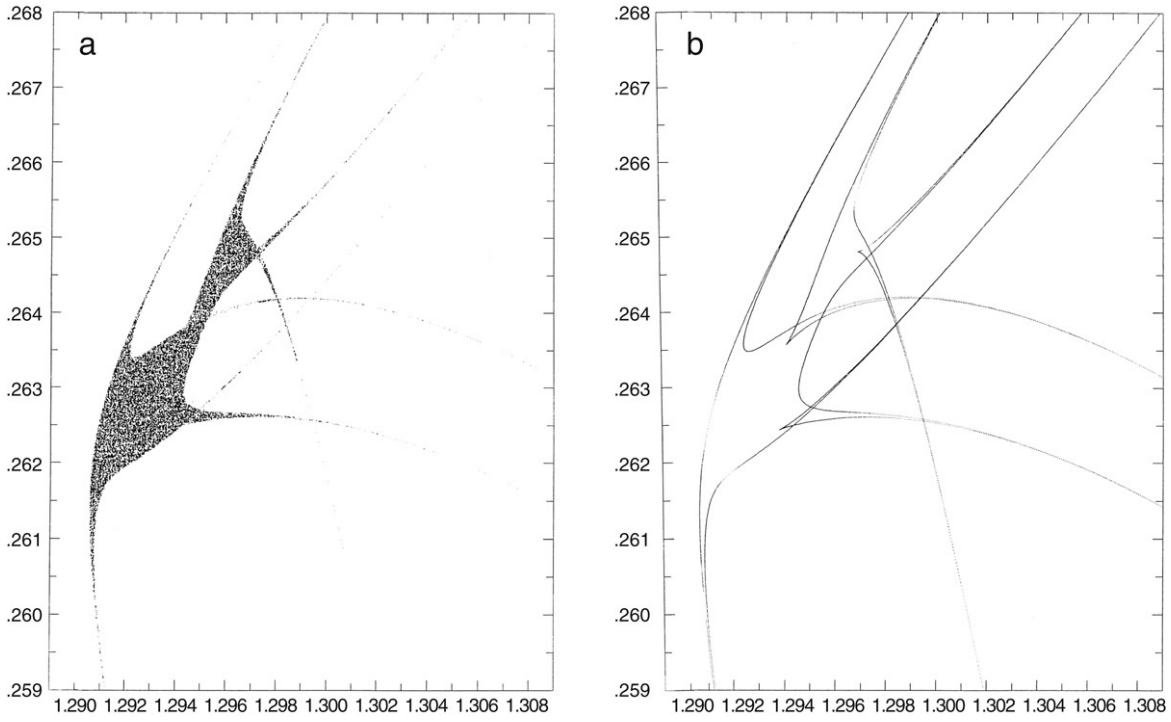

Fig. 15. (a) Irregular subwindow of period 18, determined by random searching. (b) Portions of U^+- and U^--curves in region covered by Fig. 15(a), that extend from 18(22 891), 18(22 933), 18(42 603), and 18(42 645) logistic subwindows. Horizontal scales indicate a, vertical scales indicate b.

Such pairs appear more frequently as K becomes larger, and we might consider modifying the second proposition to state that, under the given conditions, the indicated U^+- and U^--curves would bound a compound window or an almost-compound pair. Such a proposition indeed holds when $K \leq 17$, but, when $K = 18$, the first and the modified second proposition both encounter exceptions.

Fig. 15(a) shows a principal subwindow where $K = 18$, produced by random sampling over a small region after being first detected as a small irregular patch near the centre of Fig. 3(a). It might appear to be two windows whose locations happen to overlap, but Fig. 15(b), containing the segments of the $K(j_1) - K(j_4)U^+$- and U^--curves in the same region, with $j_1 = 22\,891$, $j_2 = 22\,933$, $j_3 = 42\,603$, and $j_4 = 42\,645$, shows that this is not the case. Note that $j_1 + j_4 = j_2 + j_3 = 2^K/4$. There is a four-way rotation of partners rather than two separate exchanges. Also, three of the U^+-curves possess cusps. Thus the second proposition fails. In addition, the 0-

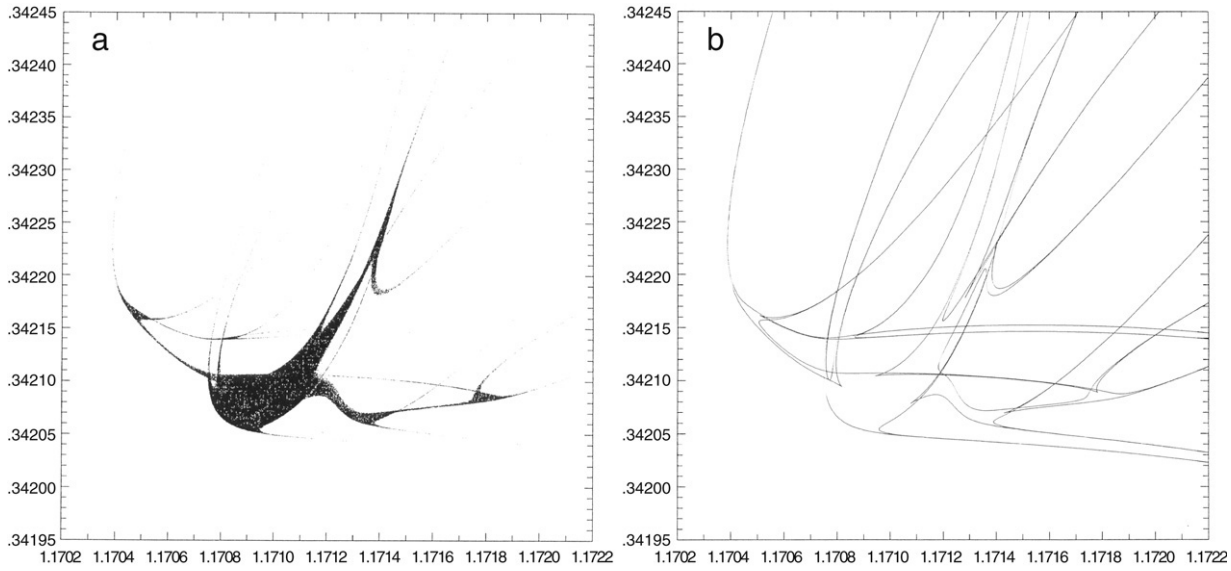

Fig. 16. (a) The same as Fig. 15(a), but for irregular subwindow of period 40. (b) The same as Fig. 15(b), but for eight logistic subwindows whose U^+- and U^--curves extend through region covered by Fig. 16(a). Horizontal scales indicate a, vertical scales indicate b.

curves extending from the $K(j_3)$ and $K(j_4)b$-windows and also from two more of the 132 b-windows with $K = 18$ do not reach 0-3-points, so that the first proposition fails.

As K becomes larger, still more shapes appear. The most intricate window that we have encountered is one of period 40. Fig. 16(a) shows the 40-subwindow, while Fig. 16(b) presents an analysis like that in Fig. 15(b), containing U^+- and U^--curves from eight b-windows. There is a complete 8-way rotation. The window of Fig. 15 seems simple by comparison.

As for street-curve intersections, we might have expected a 7-window where curves of orders two and five cross, but all that appears in Fig. 2(b) is a pair of faint streaks. Enlargement identifies it as an almost-compound pair.

The work of Mira [17] implies that windows of special shapes, including those seen in this study, are features of more general maps, but the question arises as to whether the arrangement of these windows into streets is also a general feature. We remark only that an answer can presumably be found if one is willing to perform sufficiently lengthy computations.

May [16] titled his classic paper "Simple mathematical models with very complicated dynamics." Here a system only a bit more complicated than the logistic equation has exhibited far more complicated dynamics.

Note added in proof

In this paper, I noted a frequently occurring structure in parameter space in the Hénon map [8], which I called a "compound window," and which I described as resembling a strange creature with a central body and four long antennae. Subsequently I have received a number of communications [22–25] informing me that similar structures have appeared in a number of articles, and that they have already received the apt name of "shrimps." References [22–25] and probably others should have appeared among the papers cited here, and would have appeared here if I had been aware of them at the time of submission.

Fig. 3b of my paper is nearly a copy of Fig. 7 of [25]. In view of the frequent encounters with shrimps by various authors, I feel that the principal contribution of my paper may be the recognition of long narrow bands, which I have called "window streets," composed of innumerable microscopic shrimps, and the identification of Cantor sets of readily computable smooth curves that closely approximate the window streets.

Acknowledgments

I have greatly benefited from many discussions of this work with my former colleague James A. Hansen. I thank an anonymous reviewer for bringing additional relevant studies to my attention. This work has been supported by the Large-Scale Dynamic Meteorology Programme, Lower Atmosphere Research Section, Division of Atmospheric Sciences, National Science Foundation, under Grant ATM–0216866.

References

[1] M. Benedicks, L. Carleson, The dynamics of the Hénon map, Ann. Math. 133 (1991) 73–169.
[2] J.P. Carcassès, C. Mira, M. Bosch, C. Simó, J.C. Tatjer, Crossroad area—spring area transition. (1) Parameter plane representation, Internat J. Bifur. Chaos 1 (1991) 183–196.
[3] P. Collet, J.-P. Eckmann, On the abundance of aperiodic behavior for maps of the interval, Commun. Math. Phys. 73 (1980) 115–160.
[4] J.H. Curry, On the Hénon transformation, Comm. Math. Phys. 68 (1979) 129–140.
[5] M. Feigenbaum, Quantitative universality for a class of nonlinear transformations, J. Stat. Phys. 19 (1978) 25–52.
[6] S.B. Feit, Characteristic exponents and strange attractors, Comm. Math. Phys. 61 (1978) 249–260.
[7] J. Guckenheimber, P. Holmes, Nonlinear Oscillations, Dynamical Systems, and Bifurcations of Vector Fields, Springer, New York, 1983.
[8] M. Hénon, A two-dimensional mapping with a strange attractor, Commun. Math. Phys. 50 (1976) 69–77.
[9] D.L. Hitzl, F. Zele, An exploration of the Hénon map, Physica D 14 (1985) 305–326.

[10] B.H. Hunt, J.A. Kennedy, T.-Y. Li, H.E. Nusse, SLYRB measures: natural invariant measures for chaotic systems, Physica D 170 (2002) 50–71.
[11] M.V. Jakobson, Absolutely continuous measures for one-parameter families of one-dimensional maps, Comm. Math. Phys. 81 (1981) 39–88.
[12] G. Julia, Mémoire sur l'itération des fonctions rationelles, J. Math. Pure Appl. 4 (1918) 47–245.
[13] H.A. Lauwerier, in: Chaos, A.V. Holden (Ed.), One-dimensional Iterative Maps, Princeton Univ. Press, Princeton, 1986.
[14] E.N. Lorenz, The problem of deducing the climate from the governing equations, Tellus 16 (1964) 1–11.
[15] R. Lozi, Un attracteur étrange (?) due type attracteur de Hénon, J. Phys. (Paris) 39 (1978) 9–10.
[16] R.M. May, Simple mathematical models with very complicated dynamics, Nature 261 (1976) 459–467.
[17] C. Mira, Chaotic Dynamics. From the One-Dimensional Endomorphism to the Two-dimensional Diffeomorphism, World Scientific, Singapore, 1987.
[18] C. Mira, J.P. Carcassès, M. Bosch, C. Simó, J.C. Tatjer, Crossroad area—spring area transition. (2) Foliated parameter representation, Internat J. Bifur. Chaos 1 (1991) 339–348.
[19] C. Mira, J.P. Carcassès, On the "crossroad area—saddle area" and "crossroad area—spring area" transitions, Internat. J. Bifur. Chaos 1 (1991) 641–655.
[20] L.F. Olsen, H. Degn, Chaos in biological systems, Q. Rev. Biophys. 18 (1985) 165–225.
[21] C. Simó, On the Hénon–Pomeau attractor, J. Stat. Phys. 21 (1979) 465–494.
[22] J.A.C. Gallas, Structure of the parameter space of the Hénon map, Phys. Rev. Let. 70 (1993) 2714.
[23] J.A.C. Gallas, Dissecting shrimps: results for some one-dimensional physical systems, Physica A 202 (1994) 196.
[24] C. Bonatto, J.A.C. Gallas, Y. Ueda, Chaotic phase similarities and recurrences in a damped-driven Duffling oscillator, Phys. Rev. E 77 (2008) 026217.
[25] B.R.. Hunt, J.A.C. Gallas, C. Grebogi, J.A. Yorke, H. Koçak, Bifurcation rigidity, Physica D 129 (1999) 35.